


## LETTER

# Nitrogen limitation inhibits marine diatom adaptation to high temperatures

María Aranguren-Gassis,<sup>1\*</sup>   
 Colin T. Kremer,<sup>1</sup>  
 Christopher A. Klausmeier<sup>1,2,3,4</sup>  
 and Elena Litchman<sup>1,3,4</sup>

### Abstract

Ongoing climate change is shifting species distributions and increasing extinction risks globally. It is generally thought that large population sizes and short generation times of marine phytoplankton may allow them to adapt rapidly to global change, including warming, thus limiting losses of biodiversity and ecosystem function. Here, we show that a marine diatom survives high, previously lethal, temperatures after adapting to above-optimal temperatures under nitrogen (N)-replete conditions. N limitation, however, precludes thermal adaptation, leaving the diatom vulnerable to high temperatures. A trade-off between high-temperature tolerance and increased N requirements may explain why N limitation inhibited adaptation. Because oceanic N limitation is common and likely to intensify in the future, the assumption that phytoplankton will readily adapt to rising temperatures may need to be reevaluated.

### Keywords

Adaptation, climate change, diatoms, evolutionary rescue, temperature-nutrients interaction, thermal tolerance, trade-offs, warming, evolutionary rescue.

*Ecology Letters* (2019)

## INTRODUCTION

Marine phytoplankton is responsible for about half of all carbon fixation on Earth (Field 1998). They are also key players in other biogeochemical cycles (Falkowski *et al.* 2008) and form the basis of most oceanic food webs. Phytoplankton is sensitive to global environmental change, including rising temperatures. Their productivity and diversity may decline as the oceans warm (Sarmiento *et al.* 2004; Thomas *et al.* 2012) which will have cascading effects on higher trophic levels and ecosystem functioning. Declines in productivity and diversity may be particularly severe in the tropics (Parmesan 2006; Thomas *et al.* 2012; Reusch 2013; van Dooremalen *et al.* 2013); therefore, it is especially important to investigate whether tropical phytoplankton can adapt to rising temperatures.

Evolutionary responses may help offset negative effects of rising temperature on phytoplankton. As phytoplankton have large populations, fast generation times and typically high genetic diversity (Ryneerson & Armbrust 2000, 2005), they may adapt rapidly to rising temperatures (Litchman *et al.* 2012; Padfield *et al.* 2015; Listmann *et al.* 2016; Schaum *et al.* 2017) through evolutionary rescue. Evolutionary rescue of a maladapted population occurs through the proliferation of rare, resistant individuals either initially present or arising through mutation, preventing extinction (Bell & Gonzalez 2009). Recent laboratory experiments document fast thermal adaptation: within several hundred generations, the optimum

temperature for growth and niche width increased in phytoplankton grown above their thermal optimum (Listmann *et al.* 2016; O'Donnell *et al.* 2018). However, little is known about how other stressors affect thermal adaptation (Boyd & Hutchins 2012; Boyd *et al.* 2015; Baker *et al.* 2018).

Because many parts of the ocean are nutrient-limited (Moore *et al.* 2013), and warming is often associated with decreased nutrient availability (Sarmiento *et al.* 2004), it is likely that phytoplankton adapting to rising temperatures will also experience nutrient limitation. We know of no published studies that look at the interactive effects of high temperature and nutrient limitation on phytoplankton adaptation. Thermal adaptation can increase the nutrient requirements of phytoplankton (Baker *et al.* 2018), suggesting that lower nutrient levels could affect the potential for phytoplankton to adapt to high temperatures. If nutrient limitation impedes thermal adaptation, phytoplankton biomass and diversity may decline more severely than predicted for nutrient-replete conditions.

We explore whether N-limitation affects the ability of marine phytoplankton to adapt to warming by evolving a tropical marine diatom at above-optimal temperatures (31 °C) under nitrogen (N)-replete vs. N-limited conditions. We characterised the thermal traits of evolved populations after ~ 100 and ~ 200 generations under the experimental conditions, including their tolerance of extreme temperatures. While none of the populations showed dramatic improvements in fitness at the selection temperature, under N-replete conditions the diatom gained the ability to survive previously lethal high

<sup>1</sup>W. K. Kellogg Biological Station, Michigan State University, Hickory Corners, MI 49060, USA

<sup>2</sup>Department of Plant Biology, Michigan State University, East Lansing, MI 48824, USA

<sup>3</sup>Ecology, Evolutionary Biology, and Behavior Graduate Program, Michigan State University, East Lansing, MI 48824, USA

<sup>4</sup>Department of Integrative Biology, Michigan State University, East Lansing, MI 48824, USA

\*Correspondence and present address: Campus Lagoas-Marcosende, University of Vigo, Vigo, Pontevedra 36310, Spain. E-mail: aranguren@uvigo.es

temperatures (34 °C), while N-limited populations remained vulnerable to that temperature.

## MATERIALS AND METHODS

Eight populations were evolved under above-optimal temperature (31 °C), four at N-replete and another four under N-limited conditions. After ~100 generations, their thermal performance curves (TPC) and tolerance to 34 °C were measured. Then, ~100 generations later (~200 generations total), the populations' tolerance to 34 °C was checked again and the TPCs of two randomly chosen 34 °C-tolerant populations were measured. To explain the experimental results, a model of competition was developed, showing the nutrient-dependent evolution of thermal tolerance.

### Culture conditions

The marine diatom in our study, *Chaetoceros simplex* strain CCMP 200 (National Center for Marine Algae and Microbiota, NCMA) was isolated from the Persian Gulf in 1977, where monthly average temperatures range between 19 and 32 °C (Shirvani *et al.* 2015) and yearly means span 26–28 °C (Boyer *et al.* 2013). Extreme temperatures can reach 16 °C and 35 °C (Nandkeolyar *et al.* 2013). At the NCMA, the strain was maintained at 24 °C until 2007, then cryopreserved by adding 12% dimethylsulfoxide (DMSO) as a cryoprotective agent, cooling cells by 1 °C per minute until –80 °C, and storing them at –137 °C.

We maintained this original culture (Box 1) for 16 weeks at 25 °C in nutrient-enriched artificial L1 seawater medium (884 µM NO<sub>3</sub><sup>–</sup>) from NCMA, modified from Guillard & Hargraves (1993), at pH of 8–8.2 and 33 psu salinity. Only the nitrate concentration was modified during subsequent experiments, establishing two experimental N-availability conditions: 884 µM NO<sub>3</sub><sup>–</sup> and 5 µM NO<sub>3</sub><sup>–</sup>. We bottlenecked the original culture using sequential dilution to reduce genetic variation as much as possible. The resulting population was grown for several days and split to form nine experimental populations. Sub-samples of each were cryopreserved in our laboratory (see above); subsequently, they are referred to as ancestral populations (Box 1).

### Evolution experiment

Eight populations were then grown at 31 °C, and one was maintained as a control at 25 °C in regular L1 medium (884 µM NO<sub>3</sub><sup>–</sup>). We chose 31 °C for the evolution experiment because it is within the range of expected annual mean temperatures for tropical seas, where current conditions range from 26 to 30 °C (Boyer *et al.* 2013) and may rise by 3 °C by 2100 (IPCC 2013, RCP 8.5). Preliminary work showed that our experimental line grew from 13 to 32 °C, with an optimum temperature of 25 °C (not shown). The 31 °C treatment exceeded the strain's optimum, yet permitted sufficient growth (0.5–0.7 per day) to complete the experiments in a reasonable time.

At 31 °C, four populations remained in regular L1 medium (884 µM NO<sub>3</sub><sup>–</sup>), while the other four received nitrogen-reduced L1 medium (5 µM NO<sub>3</sub><sup>–</sup>); we refer to these as N-replete

and N-limited conditions respectively. The N-replete concentration is extremely high relative to most natural settings, but ensures cells are not N-limited, providing a contrasting treatment that is consistent with previous studies. The N-limited treatment exceeds oligotrophic ocean N concentrations, but is on the low end of concentrations typical of areas with significant diatom presence (Bopp *et al.* 2005; Boyer *et al.* 2013). Growth rate reductions during the experiment (Fig. S2), and lower cell chlorophyll *a* content ( $t = 4.011$ ,  $P = 0.02$ ) and size ( $F = 18.86$ ,  $P < 0.001$ ) compared with the N-replete conditions, suggest that the 5 µM N treatment did limit our cultures (See Supporting Information Appendix 2 for chlorophyll *a* and cell size estimates).

Unless noted, in all subsequent experiments populations were maintained in 50 mL polycarbonate culture flasks, at 100 µmol quanta m<sup>–2</sup> s<sup>–1</sup> cool white fluorescent light on a 14/10 h day/night cycle. We gently inverted and randomly repositioned flasks daily. Every three days *c.* 10<sup>6</sup> cells (never < 6 × 10<sup>5</sup> cells) from each population were transferred to fresh media. We monitored populations by measuring *in vivo* optical density daily (436 nm wavelength absorbance) using a Shimadzu UV-2401PC spectrophotometer before and after each transfer.

When more than two biomass observations (optical density or fluorescence, depending on the experiment) within the exponential growth phase were available, we calculated population growth rates (day<sup>–1</sup>), or  $\mu$ , as the slope of the linear regression of ln(biomass) vs. time (days). Alternatively, when biomass measurements were made every 2–3 days, we calculated growth rate as  $\frac{\ln B_2 - \ln B_1}{t_2 - t_1}$ , where  $B$  is biomass and  $t$  is time (days) and the number of generations within a particular time range,  $\Delta t$ , as  $(\frac{\mu}{\ln 2})\Delta t$ . We characterised changes in the growth rates of the N-replete ( $n = 260$ ) and N-limited ( $n = 256$ ) populations throughout the experiment using linear mixed-effects models, with individual evolved populations as a random intercept effect (Fig. S2 and Table S1).

### Thermal performance curve (TPC) assays

#### Experiments

We assayed the TPCs of our populations twice during the evolution experiment. This involved pre-acclimating sub-cultures from each population to 28 °C (in-between the 25 °C control and 31 °C experimental treatment) in N-replete medium for 20 days (20–25 generations) to remove any effects of acclimation to previous temperatures (31 or 25 °C) and N levels. Subsequently, separate flasks containing N-replete medium were placed at each assay temperature, inoculated with pre-acclimated populations, and allowed to acclimate for six more days.

After ~100 generations of evolution (102–114 days, corresponding to 90–134 generations depending on the populations), we assessed the TPCs of all evolved populations and the control population. Assay temperatures were 12, 20, 25, 29, 31, 32 and 34 °C. Four replicate populations were established at each temperature in 12-well plates (experimental replicates, Box 1) by combining four 0.5 mL aliquots from the acclimated flasks with 4.5 mL of N-replete medium. These plates were then maintained at each temperature. We

measured *in vivo* chlorophyll-*a* fluorescence (excitation wavelength: 436 nm, emission wavelength: 680 nm) daily using a SpectraMax M5 microplate reader (Molecular Devices, Sunnyvale, CA, USA) to estimate the growth rate (252 estimates).

After ~200 generations of evolution (165–186 days: 194–232 generations), we characterised the TPCs of two randomly selected N-replete evolved populations that were 34 °C-tolerant (see the 34 °C challenge section below) and the control and an ancestral population. Assay temperatures were 10, 20, 25, 29, 31, 32, 34 and 35 °C, and three replicate populations were grown in 50-mL culture flasks (instead of well plates) (96 growth rate estimates). This change in protocol was to avoid unreliable data at 35 °C caused by evaporative losses in well plates (not shown); culture container type could affect growth rates by altering light availability, but does not invalidate comparisons between the evolved and control populations within a given assay. We discarded data from the final two days of this assay for two experimental replicates of the control populations due to contamination.

### Analysis

Exponential growth rates were calculated using biomass data collected over 8–10 days (see above). Prior to conducting regressions, we inspected the time series and removed observations occurring during lag or stationary growth phases, where apparent. However, at ~100 generations, the 34 °C regressions were based only on measurements from the first four days. This provided a simple means of isolating the response of the populations' dominant strain(s) from that of the rare 34 °C-tolerant strains, revealed by subsequent experiments and analyses (see section on 34 °C challenge below).

We described TPCs by fitting the double exponential model (Logan *et al.* 1976; Thomas *et al.* 2017) to our observed specific growth rates,  $\mu$ . This model assumes net growth rate is the difference between temperature-dependent birth and death, as follows:

$$\mu = b_1 e^{b_2 \cdot T} - (d_0 + d_1 e^{d_2 \cdot T}) \quad (1)$$

where  $T$  is the temperature,  $b_1$  and  $d_1$  respectively, provide the birth and death rates at 0 °C,  $b_2$  and  $d_2$  describe the increase in birth and death rates with temperature, and  $d_0$  is a temperature-independent source of mortality. For statistical convenience, we re-parameterised this equation (O'Donnell *et al.* 2018) to depend explicitly on  $T_{\text{opt}}$ :

$$\mu = \frac{d_1 d_2}{b_2} e^{b_2 \cdot T + (d_2 - b_2) T_{\text{opt}}} - (d_0 + d_1 e^{d_2 T}) \quad (2)$$

We fit (2) to observed growth rates to obtain estimates of underlying birth and death parameters (assuming normally distributed residuals and using maximum likelihood, *bbmle* package in R, Bolker & R Development Core Team 2017).

Next, we determined whether evolution significantly altered the TPCs of populations grown at 31 °C. At ~100 generations, we had eight evolved populations and one control population. Taking each evolved population, we tested whether its observed growth rates, combined with those of the control population, were better explained by a single TPC (following eqn 2), or two separate TPCs (for evolved vs. control) (Figs. S3 and S4; Table S2). In each case, we used model comparison (based on AICc, Akaike Information Criterion corrected for small sample size) to determine which model performed best. Additionally, we consider whether any detected changes are biologically meaningful, examining specific thermal traits,  $T_{\text{opt}}$  and maximum growth rate (Fig. S5). At ~200 generations, we had two evolved populations and two control populations. Rather than conducting pairwise tests, we considered whether all of the growth rates pooled were best described by a single TPC, two TPCs (for evolved vs. control), or four TPCs (allowing each population to differ) (Fig. S6; Table S3). We again used AICc comparison. When the model allowing TPC shape to differ between evolved vs. control populations out-performed a single shared TPC, we

### Box 1. Terminology used throughout the text

Original culture: *Chaetoceros simplex* population strain CCMP 200 (National Center for Marine Algae and Microbiota, NCMA) maintained at 25 °C and N-replete conditions before the experiment.

Experimental line: population obtained from sequential dilution of the original culture, that we subsequently split to form the different experimental evolved and control populations.

Evolved populations: cultures originated from eight of the aliquots of the experimental line, maintained at 31 °C and N-replete or N-limited conditions (four populations each).

Control population: culture originated from the experimental line and maintained at 25 °C and N-replete conditions. When presenting the ~200 generation TPCs, we also include the thawed ancestral population when referring to controls.

Ancestral populations: aliquots of the evolved and control populations that were cryopreserved at the beginning of the evolution experiment. The ancestral populations were thawed just before the ~200 generations assay and maintained in the N-replete medium at 25 °C.

Thermal performance curve (TPC): the relationship between growth rate and temperature.

34 °C challenge: exposing experimental populations to 34 °C and observing their growth.

Experimental replicates: each one of aliquots from the experimental populations used to estimate growth rates at the TPCs and 34 °C challenges assays.

Tolerant or intolerant strains: populations that grow (tolerant) or not (intolerant) at 34 °C. We use these terms to refer both to the populations that we have experimentally tested at 34 °C and the theoretical populations in the model.

concluded that evolution led to statistically different thermal performance curves.

### 34 °C challenge

The ~ 100 generation TPC assays included a 34 °C treatment, which tended to cause populations to first decline in abundance and then resume growing (Fig. 2b,c). We call this the ~ 100 generations 34 °C challenge. We tested the idea that these population-level patterns reflected the combined responses of abundant (but dying) strains and rare (but exponentially growing) strains by fitting a two-strain evolutionary rescue model (Gonzalez *et al.* 2013) to the observed dynamics of each replicate experimental population. Here, population dynamics follow:

$$N(t) = \phi N_0 e^{r_1 t} + (1 - \phi) N_0 e^{r_2 t} \quad (3)$$

where  $N_0$  is the total initial population size,  $\phi$  is the relative abundance of strain 1, and  $r_1$  ( $r_2$ ) is the growth rate of strain 1 (strain 2). Note that (3) collapses into the exponential growth of a single strain when either  $r_1 = r_2$  or  $\phi \rightarrow 1$ . We fit the ln-transformed version of (3) to observed ln(fluorescence) with normally distributed errors using maximum likelihood.

After ~ 200 generations (165–186 days: 194–232 generations for the N-replete populations; 128–151 generations for the N-limited populations), we again assessed the evolved populations' survival at 34 °C, as well as that of the control (25 °C) and ancestral populations (Box 1). We call this assay the ~ 200 generations 34 °C challenge, as it preceded the subsequent TPC assay. As before, pre-acclimation to 28 °C occurred prior to the 34 °C treatment imposed on all populations: evolved ( $n = 2$  replicates per population), control ( $n = 2$ ), and ancestral ( $n = 7$ ). We monitored growth daily using *in vivo* optical density; see above. Not all populations survived 34 °C; those that did, were maintained at 34 °C in N-replete medium and periodically transferred to avoid stationary phase, until we could subsequently measure their full TPCs (see above). In Fig. 2 we only show data collected before we transferred the cultures to fresh medium for the first time; however, cultures were maintained  $\geq 3$  weeks, including the failed populations, to verify that no growth occurred.

### Modelling the nutrient-dependent evolution of thermal tolerance

To investigate a mechanism that might explain our experimental results, we constructed a model of competition between two hypothetical strains of *Chaetoceros simplex* with distinct phenotypes. Specifically, we assume that investment in protective mechanisms enables growth at high temperatures but increases nitrogen requirements (Baker *et al.* 2018). We then explored whether N-limitation affects the ability of an initially rare strain that invests in increased protection (enabling it to grow at 34 °C) to invade a population dominated by a less protected strain, when both compete in a 31 °C environment.

#### Model structure

In this model, change in the abundance  $N_i$  of a particular strain  $i$  depends on the difference between its birth rate  $b$  and death rate  $d$ , following:

$$\frac{dN_i}{dt} = (b(p_i, R_1, R_2, T) - d(p_i, T)) \times N_i \quad (4)$$

where both rates depend on temperature  $T$  and strain-specific levels of investment in protection,  $p_i$ . Birth rate also depends on the availability of two essential resources ( $R_1$  and  $R_2$ ). We considered  $R_1$  to represent nitrogen, the focal nutrient in our experiments, while  $R_2$  is another potentially limiting resource (e.g. phosphorus or light).

This formulation represents a modified version of the double exponential model (2) described previously (Logan *et al.* 1976; Thomas *et al.* 2017; O'Donnell *et al.* 2018). Here, we define the birth term specifically as follows:

$$b(p_i, R_1, R_2, T) = b_1 \times \text{Exp}(b_2 \times T) \times \text{Min} \left[ \frac{v_1}{q_0 + q_1 \times p_i} \left( \frac{R_1}{R_1 + k_1} \right), \frac{v_2}{q_2} \left( \frac{R_2}{R_2 + k_2} \right) \right] \quad (5)$$

The first components of (5) drive an exponential increase in birth rate with temperature (for  $b_2 > 0$ ). However, this term is constrained by whichever of  $R_1$  and  $R_2$  is most limiting to growth, following Liebig's law of the minimum, and assuming Monod uptake kinetics. Here,  $v_1$  and  $v_2$  determine maximum uptake rates for the two resources,  $k_1$  and  $k_2$  set the half-saturation constants of the Monod curves, and  $q$  parameters define the quota (how much of  $R_1$  or  $R_2$  is required to produce one unit of biomass  $N$ ). A strain's quota for  $R_1$  (nitrogen) has some baseline value  $q_0$  if it does not invest in protection at all (i.e. if  $p_i = 0$ ); however, the nitrogen quota increases with investment in protection (i.e. as  $p_i$  increases) scaled by the  $q_1$  coefficient. Finally, we note that the growth of a strain can be limited by a particular resource either when: (1) the resource is low (such that  $R/(R + k)$  is very small), or (2) both resources are plentiful, but one is consumed more slowly than the other (for example, if  $v_1$  is much larger than  $v_2$ , the uptake of  $R_2$  might limit growth even when  $R_2$  is abundant).

The temperature-dependent death term consists of:

$$d(p_i, T) = \frac{d_1}{p_i} \times \text{Exp}(d_2 \times T) \quad (6)$$

where death rate increases exponentially with temperature (Thomas *et al.* 2017) but  $d_1$ , a strain's baseline mortality rate at  $T = 0$ , is scaled by the protection term  $p_i$ . Consequently, strains that invest more in protection reduce their death rate, allowing them to survive at higher temperatures. Overall, changes in each strain's abundance depend on the difference between its birth (5) and death (6) rates, given current temperature and resource levels.

Resources are continuously depleted as both strains consume and convert resources into biomass, scaled by their quotas:

$$\frac{dR_1}{dt} = - \sum_{i=1}^n (q_0 + q_1 \times p_i) \times b(p_i, R_1, R_2, T) \times N_i \quad (7)$$

$$\frac{dR_2}{dt} = - \sum_{i=1}^n q_2 \times b(p_i, R_1, R_2, T) \times N_i$$

The total amount of each resource is determined by the quantity supplied in the growth medium, imposing the initial conditions:  $R_1(0) = R_{in,1}$  and  $R_2(0) = R_{in,2}$ . Together, eqns (4)

and (7) define our model. All parameters are listed in Table S4; model parameterisation is described in Supporting Information Appendix 1.

We further tailored our model to the evolution experiment by imposing semi-continuous culture dynamics, simulating the periodic transfer and dilution of populations by regularly perturbing the state variables of our model with a fixed period of  $\tau$  (three days). At each perturbation, total population size ( $N_1 + N_2$ ) was reduced by a constant fraction  $\rho$ , without altering the relative abundance of each strain. Concentrations of each resource were simultaneously restored to  $R_{in,1}$  and  $R_{in,2}$ , then populations grew and depleted resource levels for another  $\tau$  days. This competitive regime selectively favors the strain with the highest relative abundance at the end of each period, despite regularly decreasing total abundances. Model results were obtained numerically using Mathematica v11.1.1.0 (Wolfram Research).

### C : N elemental analyses

We measured the elemental composition of the two 34 °C-tolerant populations (Fig. 1c), and the control and ancestral populations, at different temperatures. From each culture during exponential growth, we filtered 10–20 mL duplicate subsamples onto pre-combusted GF/F filters. The filters were

then dried at 60 °C for 24 h, packed in aluminium tins and kept in a desiccator. Blanks were 10–20 mL of the medium filtered and processed as other samples. Particulate C and N were measured with a CHN analyzer (Costech ECS 4010, Sollins *et al.* 1999) and ratios were calculated from weight percentage of each element after the subtraction of the corresponding blank. We used a general additive model (GAM) through the *mgcv* package in [R] to describe changes in C : N ratio across the range of temperatures where both the controls (25 °C control and ancestral) and the evolved populations grew (20 to 32 °C). Our model allowed for smoothed relationships between C : N and temperature, which varied by the evolutionary history of the populations (evolved 34 °C-tolerant or control 34 °C-intolerant), while testing for a difference in the mean C : N of the tolerant and intolerant populations. This analysis included 30 C : N values for the evolved populations and 30 for the control populations.

## RESULTS

### Thermal performance curves (TPCs)

At ~ 100 generations, we saw limited evidence of changes in the TPCs of evolved populations (Fig. 1a,b). In four of the eight comparisons a single TPC described variation in growth

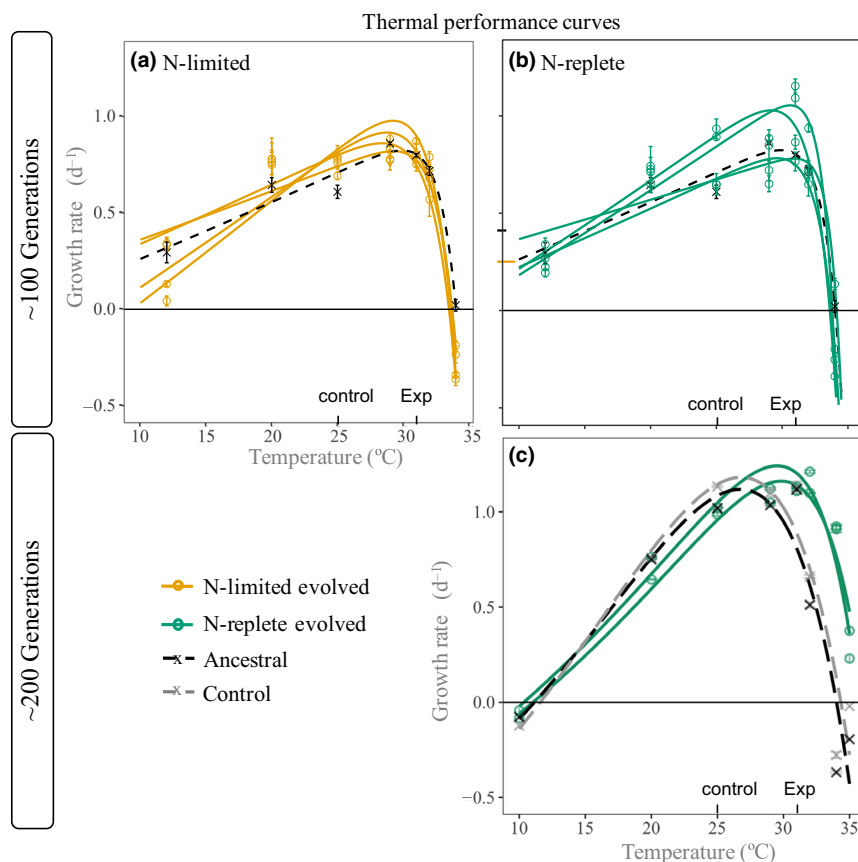


**Figure 1** Thermal performance curves at ~ 100 and ~ 200 generations. Thermal performance curves after ~ 100 generations, comparing populations evolved at 31 °C and (a) N-limited (yellow, o) or (b) N-replete (green, o) with a control (grey, x) kept at 25 °C and replete N. (c) Thermal performance curves for two of the N-replete 34 °C-tolerant evolved populations and the 25 °C control and ancestral (black, x) populations (which cannot tolerate 34 °C). Error bars are 95% confidence intervals.

rate with temperature as well as or better than models allowing the evolved and control populations to have separate TPCs (see Table S2; Figs S3 and S4). Considering specific traits, a few populations had elevated maximum growth rates (Fig. S5), but the optimum temperatures of evolved populations were not meaningfully different from the controls (confidence intervals overlap). So, while distinct control vs. evolved TPCs were statistically supported in four out of eight TPCs comparisons, the biological significance of these differences was limited in aspects such as optimum temperature.

However, after ~200 generations of evolution (Fig. 1c), the TPCs of two focal thermo-tolerant populations (evolved at 31 °C under N-replete conditions) differed significantly from those of the ancestral and control populations (the one TPC model had a higher AICc than the two TPC model, see Table S3, Fig. S6; likelihood ratio test  $P < 0.0001$ ). We saw no evidence that the TPCs of the control (maintained at 25 °C) and ancestral populations differed; similarly, both evolved populations had similar TPCs (the four TPC model had a higher AICc than the two TPC model, see Table S3, Fig. S6; likelihood ratio test  $P = 0.7029$ ). Evolved populations significantly increased their optimum temperatures relative to the controls (4.23 °C,  $z = 542.85$ ,  $P < 0.0001$ ; estimates from the two

TPC model), but grew slightly slower at 25 °C. This suggests a trade-off in growth at temperatures below and above the optimum (O'Donnell *et al.* 2018). The biggest differences, however, occurred at the highest temperatures. At 32 °C, evolved populations grew significantly faster than the controls ( $t = -13.39$ ,  $P < 0.001$ ,  $n = 6$ ), and at 34 and 35 °C, the controls failed to grow, while the evolved populations grew relatively quickly (Fig. 1c).

### 34 °C challenge

During the ~100 generations challenge, 14 of the 32 experimental replicates (including both N-limited and N-replete evolved populations) showed initial declines, followed by recovery and rapid growth after 4–6 days (Fig. 2b,c). These trajectories were extremely well described by a two-strain evolutionary rescue model ( $R^2$  values exceeding 0.9; Fig. S7, Table S5), supporting the hypothesis that evolved populations harboured a rare, 34 °C-tolerant strain. The model allowed us to infer the negative growth rate of the hypothesised dominant, 34 °C-intolerant strain, the positive growth rate of the rare, 34 °C-tolerant strain (Fig. 3a), and the relative abundance of each strain. Tolerant strains from the N-replete and N-limited populations had similar growth rates ( $t$ -test:

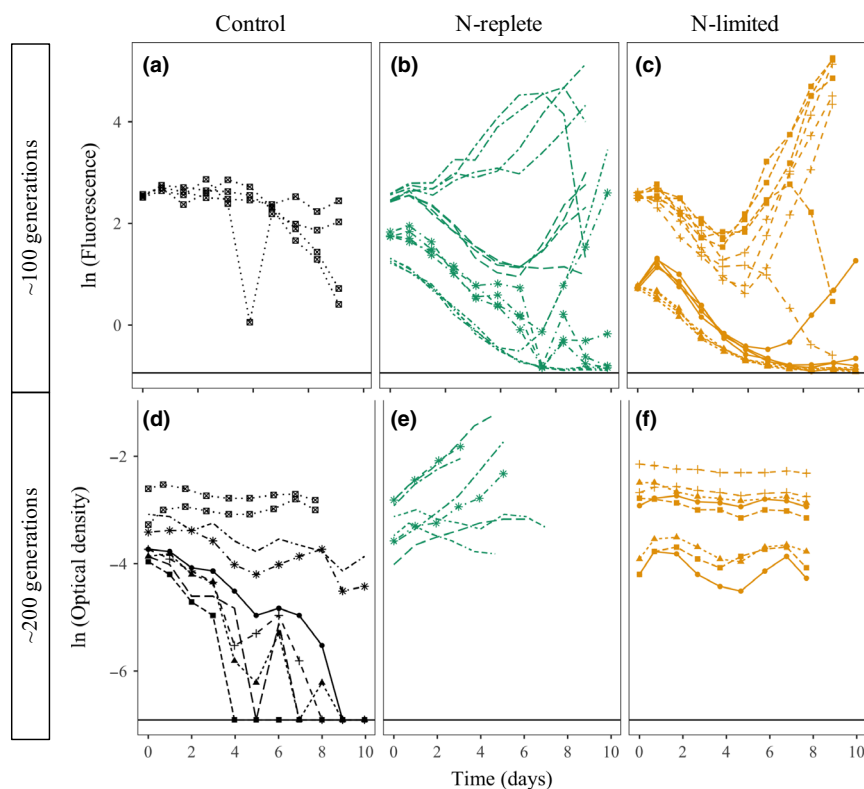


**Figure 2** Population dynamics during the two 34 °C challenges. Changes in *C. simplex* abundance over time at 34 °C are shown for all experimental replicates, after ~100 (top row) and ~200 (bottom row) generations of adaptation to 31 °C. (a) and (d) represent data for control populations, including the populations kept at 25 °C and N-replete conditions (black crossed square symbol in both panels), and those ancestral populations cryopreserved at the beginning of the evolution experiment (all the other black symbols in panel d). (b) and (e) represent N-replete (green) and (c) and (f) N-limited (yellow) conditions. Different symbols and line types represent individual experimental replicates; the horizontal black line indicates the detection threshold. The ~200 generation observations (e and f) span a shorter interval because cultures were transferred to fresh media so they could be maintained at 34 °C for multiple weeks (see methods).

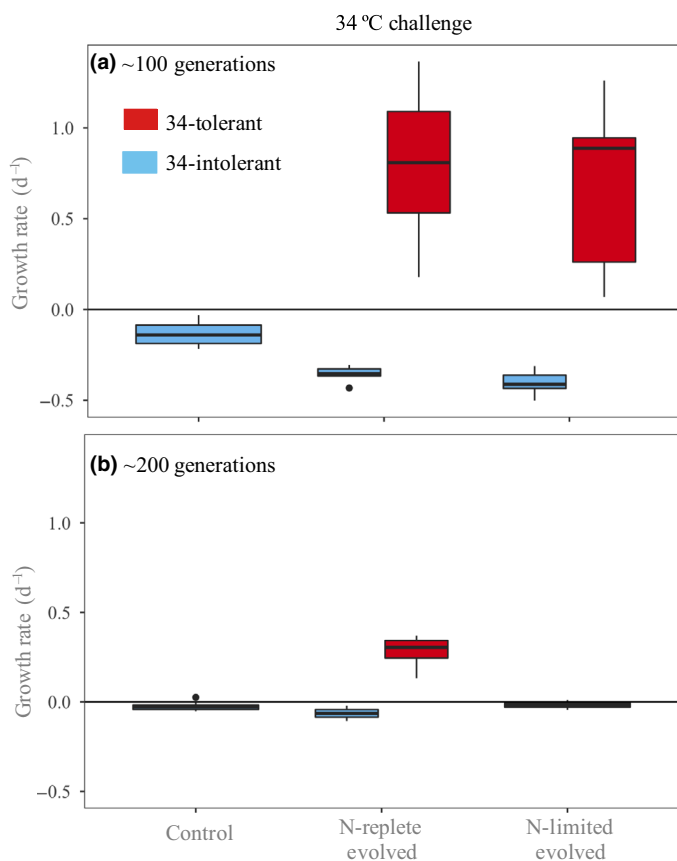


**Figure 3** 34 °C challenges. Growth rates at 34 °C after (a) ~100 generations (from daily fluorescence measurements) and (b) ~200 generations (from daily optical density measurements), identifying the high-temperature tolerant (red) and intolerant (blue) strains for each treatment. Rates at ~100 generations were estimated from each one of the experimental replicates using the evolutionary rescue model fitting (see Methods and Fig. S7).

$t = 0.371$ ;  $P = 0.715$ ; Fig. 3a), and if present, initially comprised 0.001–0.1% of most populations.

There were a few exceptions where populations either grew immediately or failed to recover, and estimated growth rates for the tolerant and intolerant strain carried the same sign (Fig. S7; Table S4). This model also underperformed when populations declined, recovered partially, then crashed, suggesting more complex dynamics occurred (e.g. N-replete evolved population 3, experimental replicate 1; Fig. S7 and Box 1 for terms). These cases were excluded from subsequent analyses and results (e.g. Fig. 3a).

In contrast, during the ~200 generations 34 °C challenge, N-replete evolved populations survived in 75% of the trials (Fig. 3b,e) and grew without delay, while N-limited evolution populations did not grow (Figs 3b and 2f).

#### Modelling the evolution of thermal tolerance

The measured TPCs of the 34 °C-tolerant and intolerant populations after ~200 generations (Fig. 4a; Table S4) provided parameters for the model we developed to explore how N supply might affect the TPCs, and hence, competition between

these two hypothesised strains. From the model, we see that when N is high, the tolerant (protected) strain grows slightly faster than the intolerant (less protected) strain at 31 °C, while at 25 °C (the ancestral condition) the strains barely differ (Fig. 4a). In contrast, N-limitation affects the intolerant strain very little, while the tolerant strain's growth rate drops; indeed, its investment in protection only becomes advantageous above 32 °C (Fig. 4b).

These changes in thermal tolerance under different N conditions lead to different competitive outcomes at 31 °C. Under N-replete conditions, the tolerant strain becomes dominant, despite its low initial abundance (Fig. 4c). However, under N-limited conditions the tolerant strain declines essentially to extinction (Fig. 4d). These patterns are qualitatively consistent with our experimental results (Fig. 2 and 3), although the model predicts fixation of the tolerant strain in < 100 generations, earlier than observed. This discrepancy in timing partly arises from the statistical parameterisation of the model, which imposes a larger difference in growth rate between strains in the model at 31 °C than may actually exist (Fig. 4a).

#### C : N elemental analyses

We found that ~200 generations of evolution altered the stoichiometry of high-temperature tolerant strains. The C : N ratios for the N-replete evolved populations (34 °C-tolerant) were significantly lower than the corresponding, intolerant controls (Fig. 5 and Table S6;  $t = -3.347$ ,  $P < 0.001$ ), supporting both our assumption of higher N demand in the high-temperature tolerant strains, and the exclusion of the tolerant strains under N-limitation that occurs in our model and experiments.

#### DISCUSSION

We evolved a tropical strain of the marine diatom *Chaetoceros simplex* under elevated temperature (31 °C) and either N-replete (typical of phytoplankton thermal adaptation experiments) or N-limited conditions (more characteristic of present and future oceans) (Fig. S1). The selection temperature was above the strain's growth optimum and within the range of the expected annual mean temperatures in the tropical seas by 2100 (IPCC 2013). We observed significant, replicated changes in phenotypic properties between the evolved and control populations, as well as between N-replete and N-limited evolving populations. However, these differences took some time to emerge, and were most apparent at temperatures above the selection temperature.

After ~100 generations at 31 °C, the evolved populations' responses to temperature were barely different from the control's (Fig. 1, Figs S3–S5, Table S2), varying only subtly at the highest temperature, 34 °C. Specifically, while control populations did not grow at 34 °C, experimental replicates of the evolved populations (both N-limited and N-replete) displayed positive growth rates at this previously lethal temperature (Fig. 2a–c). However, such growth was not always immediate (Fig. 2 and 3); many replicates showed initial declines followed by growth after 4–6 days (Fig. 2b,c), dynamics

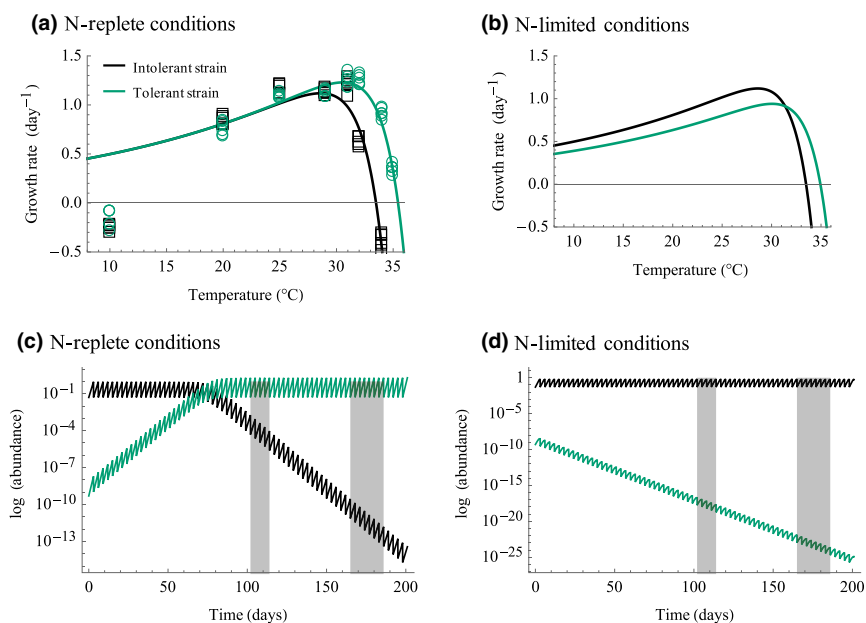


**Figure 4** Results of the competition model. Results of our empirically parameterised model of competition between high-temperature tolerant, protected (green) and intolerant, less protected (black) strains. (a, b) Thermal performance curves under (a) replete ( $R_1 = 884 \mu\text{M}$ ) and (b) limited N ( $R_1 = 5 \mu\text{M}$ ) supply. (c, d) Dynamics of competition between the strains under conditions mimicking those of the evolution experiment, (c) N-replete and (d) N-limited. Vertical grey bars indicate the timing of the  $\sim 100$  and  $\sim 200$  generation experiments.

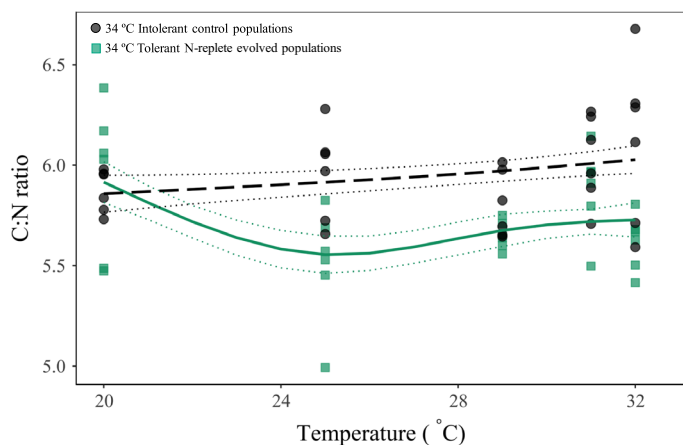


**Figure 5** C : N ratios during the thermal performance curve assay at  $\sim 200$  generations. For N-replete evolved  $34^\circ\text{C}$ -tolerant populations (green squares), and control  $34^\circ\text{C}$ -intolerant populations (black circles). Regression lines are GAMs (Generalized Additive Model) with standard error bands. The corresponding growth rates are shown in Fig. 1c.

that are highly consistent with evolutionary rescue (Gonzalez *et al.* 2013). These results support previous findings showing that persistent exposure to mildly stressful conditions (here,  $31^\circ\text{C}$ ) can lead to the evolution of enhanced tolerance of more extreme stressors (here,  $34^\circ\text{C}$ ) (Mongold *et al.* 1999; Huertas *et al.* 2011; van Dooremalen *et al.* 2013; Padfield *et al.* 2015; Listmann *et al.* 2016).

After  $\sim 200$  generations at  $31^\circ\text{C}$ , N-limited populations lost the ability to grow at  $34^\circ\text{C}$ , while this ability was dominant in at least half of the N-replete populations. Characterising the TPCs of two (randomly selected)  $34^\circ\text{C}$ -tolerant, N-replete

evolution populations showed that they differed significantly from the control (and a cryopreserved ancestral population), more than we observed at  $\sim 100$  generations (Fig. 1). Both the optimum temperature for growth and the upper thermal limit increased. These changes occurred despite surprisingly modest apparent evolutionary responses to the selection conditions: per day growth rates (a proxy for fitness, Walworth *et al.* 2016) barely rose over  $\sim 200$  generations under N-replete conditions, and did not increase under N-limited conditions (Fig. S2).

Collectively, these responses led us to hypothesise that evolved populations harboured strains with at least two distinct phenotypes that were tolerant and intolerant of  $34^\circ\text{C}$ . Note that these could reflect two phenotypically distinct groups (each containing multiple similar strains) or as few as two separate strains (given the severe bottleneck imposed prior to the evolution experiment). At  $\sim 100$  generations, the  $34^\circ\text{C}$ -tolerant strain was rare relative to the dominant, intolerant strain, but occurred across multiple evolved populations (including N-replete and N-limited) (Figs 2 and 3). By  $\sim 200$  generations, the  $34^\circ\text{C}$ -tolerant strain was dominant in N-replete populations, but seemingly absent from N-limited populations (Figs 2 and 3).

Using a mathematical model, we showed that these divergent outcomes are consistent with a scenario where high-temperature tolerance results from investing in protective mechanisms with a high N cost. This cost could arise from elevated investment in heat shock proteins, the up-regulation of proteins related to photosynthesis that increase fitness under high temperature, or other mechanisms (Hoffmann *et al.* 2003; Rousch *et al.* 2004; Toseland *et al.* 2013; Schaum *et al.* 2017). Under N-replete conditions, and at modestly

elevated temperatures (such as 31 °C), the tolerant strain is slightly favoured (has a higher growth rate), although fitness differences are small enough that exclusion of the intolerant/protected strain proceeds slowly (Fig. 4a,c). Under N-limited conditions, the N cost of investing in protection outweighs the advantage of enhanced thermal tolerance, and the tolerant strain declines (Fig. 4b,d). These model results are consistent with the results of our experiments (Figs 1 and 3), and our finding that N-replete evolved populations have lower C : N ratios (or more N per C; Fig. 5). They also indicate that resource availability can drive subtle changes in a population experiencing selection at one temperature (here, 31 °C), which may have large consequences for the population's ability to survive further increases in temperature. Such effects have not been considered in previous studies reporting adaptation to moderate warming (Mongold *et al.* 1999; Huertas *et al.* 2011; van Dooremalen *et al.* 2013; Padfield *et al.* 2015; Listmann *et al.* 2016). A trade-off between high-temperature tolerance and nitrogen demand could have tremendous implications for marine phytoplankton communities. It is often assumed that short-lived organisms with large population sizes and fast growth rates (including microbes like phytoplankton) will rapidly adapt to novel conditions resulting from climate change. We have shown that (1) populations exposed to a 6 °C increase in temperature achieved little or no obvious gains in growth rate over ~200 generations, but (2) experienced subtle yet consequential changes in their ability to survive further temperature increases, which (3) were contingent upon N availability during adaptation. This suggests that nutrient limitation may significantly impede thermal adaptation in phytoplankton. Previously, we showed that short-term N limitation reduces phytoplankton tolerance of high temperatures (Thomas *et al.* 2017); thus, N limitation may impact both ecological and evolutionary responses of phytoplankton to temperature change, enhancing their sensitivity to warming.

If N limitation inhibits adaptation to high temperatures, climate change may have greater effects on ocean primary productivity and species diversity than previously predicted, especially in warm, open oceans where nutrient limitation is common and expected to intensify (Sarmiento *et al.* 2004). Natural genetic diversity of phytoplankton populations can alleviate the effect of N limitation if better adapted genotypes to both stressors (warming and nutrient limitation) are present in the population. However, the results of the present work and others (Baker *et al.* 2018) suggest that trade-offs between adaptation to high temperatures and resource limitation may be general, constraining the response to selection in phytoplankton. Declines in species richness may lead to decreased productivity (Cermeño *et al.* 2016). More studies comparing low vs. high diversity populations are needed, but in all cases, strains or species favoured by novel conditions may have different growth rates and functional traits, altering the structure and functioning of communities. The dependence of high-temperature adaptation on nutrient availability and consequent changes in elemental stoichiometry may have broad implications for biogeochemical cycles and ecosystem functioning.

Because N limitation is common in the ocean, the assumption that phytoplankton will readily adapt to rising temperatures needs to be reevaluated. Our results show, for the first

time, that nutrient limitation may affect not only ecological but also evolutionary responses of organisms to changing climate, potentially exacerbating the effects of warming.

## ACKNOWLEDGEMENTS

We thank J.L. Herrera for help with programming and statistics, P. Woodruff, A. Hutchens and K. Shchapov for laboratory assistance and P. Wilburn for inspiring comments. We also thank the anonymous reviewers for helpful comments and suggestions. MAG was funded by a Xunta de Galicia postdoctoral fellowship. This work was funded by NSF grant OCE-1638958 to EL and CAK and is Kellogg Biological Station contribution number 2015.

## AUTHORSHIP

MAG and EL designed the experiments and discussed the data. MAG, EL and CTK wrote the manuscript and CAK commented on it. MAG performed the experiments and collected the data, which MAG and CTK analysed. CAK and CTK designed and analysed the model and discussed the model results.

## DATA AVAILABILITY STATEMENT

The data and scripts supporting the results will be archived in the GitHub repository <https://github.com/MariaArangurenGassis/PhytoEvolutionPaper2019> (data will be publicly available upon publication; <https://doi.org/10.6084/m9.figshare.8858003>).

## REFERENCES

- Baker, K.G., Radford, D.T., Evenhuis, C., Kuzhiumparam, U., Ralph, P.J. & Doblin, M.A. (2018). Thermal niche evolution of functional traits in a tropical marine phototroph. *J. Phycol.*, 54, 799–810.
- Bell, G. & Gonzalez, A. (2009). Evolutionary rescue can prevent extinction following environmental change. *Ecol. Lett.*, 12, 942–948.
- Bolker, B. & R Development Core Team (2017). *bbmle: Tools for general maximum likelihood estimations*. R package version 1.0.20. <https://CRAN.R-project.org/package=bbmle>.
- Bopp, L., Aumont, O., Cadule, P., Alvain, S. & Gehlen, M. (2005). Response of diatoms distribution to global warming and potential implications: A global model study. *Geophys. Res. Lett.*, 32, 1–4.
- Boyd, P.W. & Hutchins, D.A. (2012). Understanding the responses of ocean biota to a complex matrix of cumulative anthropogenic change. *Mar. Ecol. Prog. Ser.*, 470, 125–135.
- Boyd, P.W., Dillingham, P.W., McGraw, C.M., Armstrong, E.A., Cornwall, C.E., Feng, Y.-Y. *et al.* (2015). Physiological response of a Southern Ocean diatom to complex future ocean conditions. *Nat. Clim. Change.*, 6, 207–213.
- Boyer, T.P., Antonov, J.I., Baranova, O.K., Coleman, C., Garcia, H.E., Grodsky, A. *et al.* (2013). World Ocean Database 2013, NOAA Atlas NESDIS 72, (eds Levitus, S. & Mishonov, A.). Technical Ed., Silver Spring, MD, pp 209.
- Cermeño, P., Chouciño, P., Fernández-Castro, B., Figueiras, F.G., Maraño, E., Marrasé, C. *et al.* (2016). Marine primary productivity is driven by a selection effect. *Front. Mar. Sci.*, 3, 173.
- van Dooremalen, C., Berg, M.P. & Ellers, J. (2013). Acclimation responses to temperature vary with vertical stratification: implications for vulnerability of soil-dwelling species to extreme temperature events. *Glob. Change Biol.*, 19, 975–984.

- Falkowski, P.G., Fenchel, T. & Delong, E.F. (2008). The microbial engines that drive Earth's biogeochemical cycles. *Science*, 320, 1034–1039.
- Field, C.B. (1998). Primary production of the biosphere: integrating terrestrial and oceanic components. *Science*, 281, 237–240.
- Gonzalez, A., Ronce, O., Ferriere, R. & Hochberg, M.E. (2013). Evolutionary rescue: an emerging focus at the intersection between ecology and evolution. *Philos. Trans. R. Soc. Lond., B, Biol. Sci.*, 368, 20120404.
- Guillard, R.R.L. & Hargraves, P.E. (1993). *Stichochrysis immobilis* is a diatom, not a chrysophyte. *Phycologia*, 32, 234–236.
- Hoffmann, A.A., Sørensen, J.G. & Loeschcke, V. (2003). Adaptation of *Drosophila* to temperature extremes: bringing together quantitative and molecular approaches. *J. Therm. Biol.*, 28, 175–216.
- Huertas, I.E., Rouco, M., Lopez-Rodas, V. & Costas, E. (2011). Warming will affect phytoplankton differently: evidence through a mechanistic approach. *Proc. R. Soc. B Bio. Sci.*, 278, 3534–3543.
- IPCC (2013). Climate change 2013: The physical science basis. In: *Contribution of Working Group I to the Fifth Assessment Report of the Intergovernmental Panel on Climate Change* (eds Stocker, T.F., Qin, D., Plattner, G.K., Tignor, M., Allen, S.K., Boschung, J., Nauels, A., Xia, Y., Bex, V. & Midgley, P.M.). Cambridge University Press, Cambridge (UK) and New York (NY, USA), pp. 1535.
- Listmann, L., LeRoch, M., Schlüter, L., Thomas, M.K. & Reusch, T.B.H. (2016). Swift thermal reaction norm evolution in a key marine phytoplankton species. *Evol. Appl.*, 9, 1156–1164.
- Litchman, E., Edwards, K.F., Klausmeier, C.A. & Thomas, M.K. (2012). Phytoplankton niches, traits and eco-evolutionary responses to global environmental change. *Mar. Ecol. Prog. Ser.*, 470, 235–248.
- Logan, J.A., Wollkind, D.J., Hoyt, S.C. & Tanigoshi, L.K. (1976). An analytical model for description of temperature dependent rate phenomena in arthropods. *Environ. Entomol.*, 5, 1133–1140.
- Mongold, J.A., Bennett, A.F. & Lenski, R.E. (1999). Evolutionary adaptation to temperature. VII. Extension of the upper thermal limit of *Escherichia coli*. *Evolution*, 53, 386–394.
- Moore, C.M., Mills, M.M., Arrigo, K.R., Berman-Frank, I., Bopp, L., Boyd, P.W. *et al.* (2013). Processes and patterns of oceanic nutrient limitation. *Nat. Geosci.*, 6, 701–710.
- Nandkeolyar, N., Raman, M., Kiran, G.S. & Ajai (2013). Comparative analysis of sea surface temperature pattern in the Eastern and Western Gulfs of Arabian Sea and the Red Sea in recent past using satellite data. *Int. J. Oceanogr.*, 2013, 1–16.
- O'Donnell, D.R., Hamman, C.R., Johnson, E.C., Kremer, C.T., Klausmeier, C.A. & Litchman, E. (2018). Rapid thermal adaptation in a marine diatom reveals constraints and trade-offs. *Glob. Change Biol.*, 24(10), 4554–4565.
- Padfield, D., Yvon-Durocher, G., Buckling, A., Jennings, S. & Yvon-Durocher, G. (2015). Rapid evolution of metabolic traits explains thermal adaptation in phytoplankton. *Ecol. Lett.*, 19, 133–142.
- Parmesan, C. (2006). Ecological and evolutionary responses to recent climate change. *Annu. Rev. Ecol. Evol. S.*, 37, 637–669.
- Reusch, T.B.H. (2013). Climate change in the oceans: evolutionary versus phenotypically plastic responses of marine animals and plants. *Evol. Appl.*, 7, 104–122.
- Rousch, J.M., Bingham, S.E. & Sommerfeld, M.R. (2004). Protein expression during heat stress in thermo-intolerant and thermo-tolerant diatoms. *J. Exp. Mar. Biol. Ecol.*, 306, 231–243.
- Rynearson, T.A. & Armbrust, E.V. (2000). DNA fingerprinting reveals extensive genetic diversity in a field population of the centric diatom. *Limnol. Oceanog.*, 45, 1329–1340.
- Rynearson, T.A. & Armbrust, E.V. (2005). Maintenance of clonal diversity during a spring bloom of the centric diatom *Ditylum brightwellii*. *Mol. Ecol.*, 14, 1631–1640.
- Sarmiento, J.L., Slater, R., Barber, R., Bopp, L., Doney, S.C., Hirst, A.C. *et al.* (2004). Response of ocean ecosystems to climate warming. *Global Biogeochem. Cycles.*, 18, GB3003.
- Schaum, C.E., Barton, S., Bestion, E., Buckling, A., Garcia-Carreras, B., Lopez, P. *et al.* (2017). Adaptation of phytoplankton to a decade of experimental warming linked to increased photosynthesis. *Nat. Ecol. Evol.*, 1, 1–7.
- Shirvani, A., Nazemosadat, S.M.J. & Kahya, E. (2015). Analyses of the Persian Gulf sea surface temperature: prediction and detection of climate change signals. *Arab. J. Geosci.*, 8, 2121–2130.
- Sollins, P., Glassman, C., Paul, E.A., Swanston, C., Lajtha, K. & Heil, J. (1999). Soil carbon and nitrogen: pools and fractions. In: *Standard Soil Methods for Long-term Ecological Research* (eds Robertson, G.P., Coleman, D.C., Bledsoe, C.S. & Sollins, P.). Oxford University Press, New York (New York, USA), pp. 89–105.
- Thomas, M.K., Kremer, C.T., Klausmeier, C.A. & Litchman, E. (2012). Global pattern of thermal adaptation in marine phytoplankton. *Science*, 338, 1085–1088.
- Thomas, M.K., Aranguren-Gassis, M., Kremer, C.T., Gould, M.R., Anderson, K., Klausmeier, C.A. *et al.* (2017). Temperature–nutrient interactions exacerbate sensitivity to warming in phytoplankton. *Glob. Change Biol.*, 23, 3269–3280.
- Toseland, A., Daines, S.J., Clark, J.R., Kirkham, A., Strauss, J., Uhlig, C. *et al.* (2013). The impact of temperature on marine phytoplankton resource allocation and metabolism. *Nat. Clim. Change*, 3, 979–984.
- Walworth, N.G., Lee, M.D., Fu, F.X., Hutchins, D.A. & Webb, E.A. (2016). Molecular and physiological evidence of genetic assimilation to high CO<sub>2</sub> in the marine nitrogen fixer *Trichodesmium*. *P Natl Acad. Sci. USA*, 113(47), E7367–E7374.

## SUPPORTING INFORMATION

Additional supporting information may be found online in the Supporting Information section at the end of the article.

Editor, Amanda Bates

Manuscript received 25 February 2019

First decision made 23 March 2019

Second decision made 14 June 2019

Manuscript accepted 2 July 2019